Quasistationary fluid motions in magnetized neutron stars

IOP Conf. Series: Journal of Physics: Conf. Series **1038** (2018) 012009 doi:10.1088/1742-6596/1038/1/012009

Quasistationary fluid motions in magnetized neutron stars

D D Ofengeim, M E Gusakov, and E M Kantor

Ioffe Institute, 26 Politekhnicheskaya Street, St. Petersburg 194021, Russia

E-mail: ddofengeim@gmail.com

Abstract. In the recent work by Gusakov, Kantor & Ofengeim [Phys. Rev. D 96, 103012 (2017)] a new method to calculate the quasistationary evolution of magnetic field in the core of a neutron star was proposed. Here we further develop it, focusing on a simple case of neutron-proton-electron (npe) core composition with purely poloidal magnetic field B. We find that the meridional flow of the npe-fluid can be unexpectedly large. We estimate the typical timescale τ of the field evolution due to dragging of the magnetic field lines by this flow and show that τ can be as small as $\sim (100 - 1000)$ yr for magnetars with $B \sim 10^{16}$ G.

1. Introduction

One of the most intriguing problems of neutron star (NS) physics is understanding of interrelation between various classes of neutron stars with often very different surface magnetic fields. What are the factors that make their fields so distinct? A lot of effort has been devoted to answer this question. Clearly, the magnetic field at the surface should be related in some way to the magnetic field in the internal layers of NSs. Up until now the main body of research has been concentrated on the magnetic field evolution in the crust (e.g., [1]). The evolution in the core has received less attention partly because such an analysis is substantially more complicated, while the physics involved is not well understood, and partly because it is often believed (but see, e.g., [2]) that the typical timescales of the magnetic field evolution in the core are much larger than those in the crust (see, e.g., recent papers [2], [3], and [4] for different approaches to the problem). This work continues our studies of the magnetic field evolution in the NS core. Recently we formulated a self-consistent approach to this problem [5]. In the present work we further develop it and apply the ideas from [5] to the simplified case of normal (nonsuperfluid and nonsuperconducting) NS core, composed of only three particle species (neutrons n, protons p, and electrons e). The magnetic field in the core is taken to be axisymmetric and purely poloidal. Note that purely poloidal configuration of the magnetic field in the whole star is known to be unstable (e.g. [6]; [4] and refs. therein). Stable models seem to have mixed poloidal-toroidal structure (in principle, the toroidal component can be localized in the stellar crust). The formalism presented below can be applied to magnetic fields with toroidal component in the core, but such an analysis is beyond the scope of this short paper.

2. Evolution equations

Let $n_a(r)$ and $\mu_a(r)$ be the unperturbed (i.e., in the absence of the magnetic field) number densities and chemical potentials of particle species $a = n$, p, e, respectively. Since we assume

that an unperturbed star is non-rotating, $n_a(r)$, $\mu_a(r)$ and other unperturbed quantities depend on the radial coordinate only (hereafter we use the spherical coordinates r, θ, φ with the origin at the stellar centre). These dependencies follow from the solution to the Tolman-Oppenheimer-Volkoff equations. For a degenerate matter of NS core we have $\sum_a \mu_a n_a = \varepsilon + P$, where $\varepsilon = \rho c^2$ and P are the energy density and pressure, respectively.

An applied magnetic field drives the system out of diffusive and beta-equilibrium, which disturbs chemical potentials, $\delta\mu_a \sim (B^2/P)\mu_a$, and induces motions of each particle species a with the velocities $\boldsymbol{u}_a$. For realistic internal fields, $B \lesssim 10^{16}$ G [7], we have $\delta\mu_a \ll \mu_a$. It is convenient to define a total flow velocity, $\boldsymbol{U} = \sum_a \mathscr{X}_a \boldsymbol{u}_a$, where $\mathscr{X}_a = \mu_a n_a/(\varepsilon + P)$, and the diffusion velocities $\boldsymbol{w}_a = \boldsymbol{u}_a - \boldsymbol{U}$. For an npe NS core $\mathscr{X}_n = n_n/n_b$, where $n_b = n_n + n_p$ is the total baryon number density, $\mathscr{X}_e = \hbar c(3\pi^2 n_e)^{1/3} n_e/(\varepsilon + P)$, and $\mathscr{X}_p = 1 - \mathscr{X}_n - \mathscr{X}_e$. For future convenience we also express the electric field $\boldsymbol{E}$ in the form: $\boldsymbol{E} = \boldsymbol{E}_{\rm com} - \boldsymbol{U} \times \boldsymbol{B}/c$, where $\boldsymbol{E}_{\rm com}$ is the electric field in the frame comoving with the fluid ($\boldsymbol{U} = 0$).

To simplify analysis of the magnetic field evolution in the NS core, we, following the papers [4, 5, 8], neglect the effects of General relativity, although the equation of state is assumed to be relativistic. We also assume that NS interiors are thermally relaxed (the evolution is sufficiently slow) so that the (redshifted) core temperature is uniform, $\widetilde{T} = T\sqrt{g_{00}}$, where g_{00} is the time component of the metric tensor, and T is the local temperature. Then, in the quasistationary approximation, the evolution equations can be written as [5]

$$e_a n_a \left(\boldsymbol{E}_{\rm com} + \frac{\boldsymbol{w}_a}{c} \times \boldsymbol{B}\right) = n_a \boldsymbol{\nabla}\delta\mu_a + \sum_b J_{ab}\left(\boldsymbol{w}_a - \boldsymbol{w}_b\right), \tag{1a}$$

$$\operatorname{div} n_n\left(\boldsymbol{U} + \boldsymbol{w}_n\right) = -\operatorname{div} n_p\left(\boldsymbol{U} + \boldsymbol{w}_p\right) = -\operatorname{div} n_e\left(\boldsymbol{U} + \boldsymbol{w}_e\right) = \lambda\Delta\mu, \tag{1b}$$

$$e n_e\left(\boldsymbol{w}_p - \boldsymbol{w}_e\right) = \frac{c}{4\pi}\operatorname{rot}\boldsymbol{B}, \tag{1c}$$

$$\frac{\partial \boldsymbol{B}}{\partial t} = -c\operatorname{rot}\boldsymbol{E}_{\rm com} + \operatorname{rot}(\boldsymbol{U} \times \boldsymbol{B}). \tag{1d}$$

Here $J_{ab}(\boldsymbol{w}_a - \boldsymbol{w}_b)$ is the friction force between the species a and b, and $\lambda\Delta\mu$ (with $\Delta\mu \equiv \delta\mu_p + \delta\mu_e - \delta\mu_n$) is the rate of non-equilibrium Urca processes, which is valid under assumption $\Delta\mu \ll kT$ (k is the Boltzmann constant)[1]. The coefficients J_{ab} and λ are taken from [9] and [10, 11], respectively. Generally, they depend on n_a and T and, therefore, on the radial coordinate r. Since $J_{np}, J_{ep} \gg J_{ne}$, the latter quantity is neglected below. For simplicity we neglect perturbations of gravitational force in equation (1a) (Cowling approximation). However, it could be easily accounted for if necessary [5]. Below we shall demonstrate how to find $\boldsymbol{U}$ and $\boldsymbol{E}_{\rm com}$ from equations (1a) — (1c) for a given $\boldsymbol{B}$. Knowledge of these quantities opens a possibility to self-consistently study the evolution of the magnetic field with time using the Faraday equation (1d).

The calculation of $\boldsymbol{U}$ and $\boldsymbol{E}_{\rm com}$ proceeds in 5 steps. The *first step* consists in obtaining $\Delta\mu$ and $\delta\mu_n$ from equation (1a), summed over the index a,

$$n_b \boldsymbol{\nabla}\delta\mu_n + n_e \boldsymbol{\nabla}\Delta\mu = \frac{1}{4\pi}\operatorname{rot}\boldsymbol{B} \times \boldsymbol{B} = \boldsymbol{f}_L, \tag{2}$$

where $\boldsymbol{f}_L$ is the Lorentz force density acting on the fluid. In an axisymmetric and poloidal magnetic field we are interested in here one has $f_{L\varphi} = 0$ and the solution to (2) can be written as [5]

$$\begin{pmatrix} \hat{\mathbf{P}}_l \Delta\mu \\ \hat{\mathbf{P}}_l \delta\mu_n \end{pmatrix} = \begin{pmatrix} n_e & n_b \\ n_e' & n_b' \end{pmatrix}^{-1} \begin{pmatrix} r\hat{\mathbf{P}}_l \int_0^\theta f_{L\theta}\mathrm{d}\theta \\ \partial_r\left(r\hat{\mathbf{P}}_l \int_0^\theta f_{L\theta}\mathrm{d}\theta\right) - \hat{\mathbf{P}}_l f_{Lr} \end{pmatrix}, \qquad l \geqslant 1, \tag{3}$$

[1] As shown in [5], the case $\Delta\mu \gtrsim kT$ can be realized only for superstrong magnetic fields $> 10^{16}$ G, which are not considered here.

where the operator $\hat{\mathbf{P}}_l(\cdot)$ extracts the l'th Legendre component of the function $(\cdot)$, i.e. $\hat{\mathbf{P}}_l(\cdot) = (2l+1)/2 \int_0^\pi (\cdot) P_l(\cos\theta) \sin\theta \mathrm{d}\theta$, where P_l is the l'th Legendre polynomial. Note that the components with $l \geqslant 1$ are independent of the neutron star temperature $\widetilde{T}$. Note also that the components $\hat{\mathbf{P}}_0 \Delta\mu$ and $\hat{\mathbf{P}}_0 \delta\mu_n$ are still left undetermined.

The *second step* consists in expressing $\boldsymbol{w}_a$ and $\boldsymbol{E}_{\mathrm{com}}$ from equations (1a) for neutrons and electrons, equation (1c), and the condition $\sum_a \mathscr{X}_a \boldsymbol{w}_a = 0$, following from the definitions of $\boldsymbol{w}_a$ and $\boldsymbol{U}$. For the diffusion velocities the result is

$$\boldsymbol{w}_n = -(1-\mathscr{X}_n)\frac{n_n}{J_{np}}\boldsymbol{\nabla}\delta\mu_n + \frac{c}{4\pi e n_e}\mathscr{X}_e \operatorname{rot}\boldsymbol{B}, \tag{4a}$$

$$\boldsymbol{w}_p = \mathscr{X}_n\frac{n_n}{J_{np}}\boldsymbol{\nabla}\delta\mu_n + \frac{c}{4\pi e n_e}\mathscr{X}_e \operatorname{rot}\boldsymbol{B}, \tag{4b}$$

$$\boldsymbol{w}_e = \mathscr{X}_n\frac{n_n}{J_{np}}\boldsymbol{\nabla}\delta\mu_n - \frac{c}{4\pi e n_e}(1-\mathscr{X}_e) \operatorname{rot}\boldsymbol{B}, \tag{4c}$$

while for the electric field

$$\boldsymbol{E}_{\mathrm{com}} = -\frac{\boldsymbol{\nabla}\delta\mu_e}{e} + \frac{cJ_{ep}}{4\pi e^2 n_e^2}\operatorname{rot}\boldsymbol{B} - \frac{\mathscr{X}_n n_n}{cJ_{np}}\boldsymbol{\nabla}\delta\mu_n \times \boldsymbol{B} + \frac{1-\mathscr{X}_e}{4\pi e n_e}\operatorname{rot}\boldsymbol{B}\times\boldsymbol{B}, \tag{5}$$

where $\delta\mu_e$ is a function of $\delta\mu_n$ and $\Delta\mu$, and is specified by choosing equation of state.

In the *third step* we derive the poloidal components of $\boldsymbol{U}$ from the continuity equations (1b) for, e.g., neutrons and protons. For poloidal $\boldsymbol{B}$ the terms with $\operatorname{rot}\boldsymbol{B}$ in equations (4) have azimuthal components only and due to axisymmetry of the system they do not contribute in (1b). This leads to the relation $\operatorname{div}\boldsymbol{U} = -(n_b'/n_b)U_r$, where the prime $'$ means d/dr. Then, employing the method from Sec. III C 1 of [5], we find

$$U_r = \frac{n_b}{n_b' n_e - n_e' n_b}\left[\operatorname{div}\left(\mathscr{X}_n\frac{n_e n_n}{J_{np}}\boldsymbol{\nabla}\delta\mu_n\right) + \lambda\Delta\mu\right], \tag{6a}$$

$$U_\theta = -\frac{1}{r n_b \sin\theta}\frac{\partial}{\partial r}\left(r^2 n_b \int_0^\theta U_r(r,\theta')\sin\theta' \mathrm{d}\theta'\right) + \frac{\xi(r)}{\sin\theta}, \tag{6b}$$

where $\xi(r)$ is an arbitrary function.

The *fourth step* consists in accounting for the fact that $U_\theta(\theta=0)=0$ and $U_\theta(\theta=\pi)=0$ for any r. The first condition is satisfied with $\xi=0$; the second one is equivalent to $\hat{\mathbf{P}}_0 U_r = 0$, or

$$\frac{1}{r^2}\frac{\mathrm{d}}{\mathrm{d}r}\left(r^2\mathscr{X}_n\frac{n_e n_n}{J_{np}}\frac{\mathrm{d}}{\mathrm{d}r}\hat{\mathbf{P}}_0\delta\mu_n\right) + \lambda\hat{\mathbf{P}}_0\Delta\mu = 0. \tag{7}$$

Using this equation together with the 0-th Legendre component of equation (2),

$$n_b(\hat{\mathbf{P}}_0\delta\mu_n)' + n_e(\hat{\mathbf{P}}_0\Delta\mu)' = \hat{\mathbf{P}}_0 f_{Lr}, \tag{8}$$

one can calculate $\hat{\mathbf{P}}_0\delta\mu_n$ and $\hat{\mathbf{P}}_0\Delta\mu$, and hence fully determine the quantities $\delta\mu_n$ and $\Delta\mu$ (see step 1). However, in order to solve equations (7) and (8) one has to specify three boundary conditions.

One of these conditions, following from the requirement of finiteness of the first term in (7), is $(\hat{\mathbf{P}}_0\delta\mu_n)'\big|_{r=0} = 0$. This condition is equivalent to $(\hat{\mathbf{P}}_0\Delta\mu)'\big|_{r=0} = 0$, since $\hat{\mathbf{P}}_0 f_{Lr}\big|_{r=0} = 0$ due to the symmetry of the system. The other two conditions should be the values of $\hat{\mathbf{P}}_0\Delta\mu$ and $\hat{\mathbf{P}}_0\delta\mu_n$ at some point in the star. Possible options for these conditions are discussed in the end of Appendix D in [5].

However, in the two limiting (yet important) cases equations (7) and (8) can be easily solved. The first is the case of low temperatures, when the second term in (7) can be neglected. Then $\hat{\mathbf{P}}_0\delta\mu_n \approx C_1$ and $\hat{\mathbf{P}}_0\Delta\mu \approx C_2 + \int_0^r \hat{\mathbf{P}}_0 f_{Lr}/n_e \mathrm{d}r$, where C_1 and C_2 are some constants. The opposite case [large temperatures; the first term in (7) can be neglected] results in $\hat{\mathbf{P}}_0\Delta\mu \approx C_1 + \int_0^r \hat{\mathbf{P}}_0 f_{Lr}/n_b \mathrm{d}r$ and $\hat{\mathbf{P}}_0\Delta\mu \approx 0$. As shown in [5], at intermediate temperatures, when both terms in equation (7) are equally important, dissipation of magnetic field due to ambipolar diffusion (driven by np friction) and due to non-equilibrium Urca processes are close to one another. According to figures 1 and 2 of [5] this occurs at the redshifted temperature $\widetilde{T} \sim (0.4 - 0.9) \times 10^8$ K, if the direct Urca process is allowed and at $\widetilde{T} \sim (5 - 10) \times 10^8$ K if it is forbidden, and substituted by the next most powerful beta-process – the modified Urca one. Since λ and J_{np} rapidly vary with $\widetilde{T}$, the range of temperatures, where both limiting solutions are inaccurate, is thin. For instance, when the direct Urca is forbidden, the low-temperature limit is already valid at $\widetilde{T} \lesssim 3 \times 10^8$ K. Similarly, the high-temperature limiting solution can be safely used at $\widetilde{T} \gtrsim 2 \times 10^9$ K.

The *fifth step* consists in solving the problem of U_φ that is easy for poloidal magnetic field. Below, let us distinguish the poloidal and toroidal parts of vectors with the superscripts (p) and (t), respectively. Then $\boldsymbol{U}^{(t)} = U_\varphi \boldsymbol{e}_\varphi$, and we already know $\boldsymbol{U}^{(p)}$, $\boldsymbol{E}^{(p)}_{\rm com}$, and $\boldsymbol{E}^{(t)}_{\rm com}$ from the steps 2 — 4. In case of $\boldsymbol{B}^{(t)} = 0$ equation (1d) splits into two equations,

$$\frac{\partial \boldsymbol{B}^{(p)}}{\partial t} = \mathrm{rot}\left(\boldsymbol{U}^{(p)} \times \boldsymbol{B}^{(p)} - c\boldsymbol{E}^{(t)}_{\rm com}\right), \qquad \frac{\partial \boldsymbol{B}^{(t)}}{\partial t} = \mathrm{rot}\left(\boldsymbol{U}^{(t)} \times \boldsymbol{B}^{(p)} - c\boldsymbol{E}^{(p)}_{\rm com}\right). \tag{9}$$

From the second of these equations we see that if, initially, $\boldsymbol{B}^{(t)} = 0$, it will remain so if $\boldsymbol{U}^{(t)} = -c(\boldsymbol{E}^{(p)}_{\rm com} + \boldsymbol{\nabla}\chi) \times \boldsymbol{B}^{(p)}/(\boldsymbol{B}^{(p)})^2$, where $\chi(r,\theta)$ is an arbitrary scalar function. Note that, as follows from (9), the evolution of the magnetic field $\boldsymbol{B} = \boldsymbol{B}^{(p)}$ in this case is independent of the toroidal velocity of the flow. Thus, applying steps 1 — 5 to a given poloidal field $\boldsymbol{B}(r,\theta)$, we can find $\partial_t \boldsymbol{B}$ and hence follow the evolution of the magnetic field with time.

However, numerical calculations (e.g., [6]; see also [4] and references therein) indicate that pure poloidal field is unstable. In the more general case of mixed poloidal-toroidal axisymmetric configuration of the magnetic field, we can derive an equation for U_ϕ from the condition $\partial_t f_{L\varphi} = 0$ [5]. Solving it, we can completely determine $\boldsymbol{U}$, so that $\partial_t \boldsymbol{B}$ could again be found from (1d).

3. Numerical example

To illustrate the results of the previous section, we consider a neutron star with the HHJ equation of state [12] and mass $M = 1.4\ \mathrm{M}_\odot$, that gives the circumferential radius $R = 12.2$ km. All the non-perturbed quantities like $n_a(r)$, $\varepsilon(r)$, etc. are obtained from the solution of the Tolman-Oppenheimer-Volkoff equations. The direct Urca process is forbidden in the whole NS volume.

We use a simple analytic model for the poloidal field $\boldsymbol{B}$ taken from [4] (their model A):

$$\boldsymbol{B} = \frac{\boldsymbol{\nabla}\Psi \times \boldsymbol{e}_\varphi}{r\sin\theta}, \qquad \Psi = B_{\max} R^2 \left(\frac{r^2}{2R^2} - \frac{3r^4}{5R^4} + \frac{3r^6}{14R^6}\right)\sin^2\theta. \tag{10}$$

Here Ψ is a magnetic flux function, $B_{\max}$ is the maximum value of the magnetic field, which is achieved in the NS centre. It is proportional to the magnetic field at the pole, $B_p = (8/35)B_{\max}$. It is the simplest model of a dipole poloidal field which is matched with a vacuum dipole magnetic field outside the star. Its configuration, as well as the direction of the Lorentz force density are shown in figure 1a.

Figures 1b,c present $\Delta\mu$ and $\delta\mu_n$ in units of $k\widetilde{T}$, derived from equation (3) adopting the low-temperature approximation to the solution of equations (7) and (8). This is a good approximation for a chosen $\widetilde{T} = 2 \times 10^8$ K. To plot the figures, we assume $B_p = 10^{14}$ G

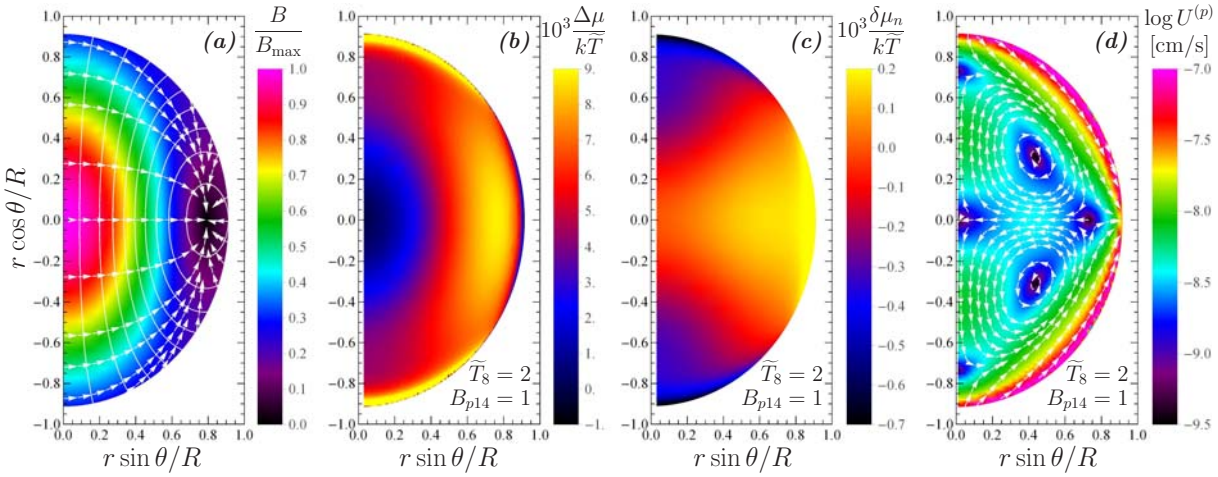

Figure 1. Properties of the NS model considered in the text. All figures show a meridional cross-section of the NS core; on each plane the left vertical axis is the symmetry axis. *(a)* The magnetic field model (equation 10). Different colors denote strength of the magnetic field in units of $B_{\max}$. Thin white lines are the field lines, arrows show direction of $\boldsymbol{f}_L$. *(b)* and *(c)* The ratios $\Delta\mu/k\widetilde{T}$ and $\delta\mu_n/k\widetilde{T}$ for $\widetilde{T} = 2\times10^8$ K and $B_p = 10^{14}$ G calculated in the low-temperature approximation (it is assumed that the direct Urca process is forbidden). *(d)* Poloidal velocity of the flow $\boldsymbol{U}^{(p)}$ for the same conditions. Arrows show direction of $\boldsymbol{U}^{(p)}$, its magnitude is shown by colors in $\log_{10}$ scale.

(corresponding to $B_{\max} \approx 4.4\times10^{14}$ G), which is a typical magnetar field [13]. Inspection of the figures reveals that, typically, $\Delta\mu \sim (n_b/n_e)\delta\mu_n$.

The ratio $\Delta\mu/kT$ was also calculated in [4] for a very similar NS model. The results of [4] are presented in the left panel of their figure 2 and differ substantially from those shown in figure 1b. The reason for the discrepancy is some approximations made in [4], which, as we argue in Appendix B of [5], are incorrect.

Figure 1d is the most interesting and it displays the poloidal flow velocity $\boldsymbol{U}^{(p)}$ derived from equations (6). The same friction coefficient J_{np} as in [4] and [5] is employed. While one could expect such a geometry of the flow for a dipole field $\boldsymbol{B}$ with the equatorial symmetry (e.g., a similar configuration was proposed in [14]), the typical velocities appear to be surprisingly large, and they grow rapidly near the crust-core interface. The reason for this behavior is easy to understand. According to (6), U_r and U_θ contain a number of terms depending on the derivatives $n_a'(r)$, $n_a''(r)$, $n_a'''(r)$, and $n_a''''(r)$. Near the crust-core interface, one has $|n_a^{(k+1)}(r)| \gtrsim (10-15)|n_a^{(k)}(r)/R|$ for $k = 0...3$, where a superscript (k) denotes k'th derivative with respect to r. As a result, for a chosen fiducial values of B_p and $\widetilde{T}$ one has $U^{(p)} \gtrsim (10-100)w_a$, because the diffusion velocities depend on the first and second derivatives $n_a'(r)$ and $n_a''(r)$ only. An actual numerical value of the ratio $U^{(p)}/w_a$ depends on B_p and $\widetilde{T}$, but for $B_p \gtrsim 10^{13}$ G the flow velocity $U^{(p)}$ is always much larger than w_a. The second interesting observation following from the discussion above is that $U^{(p)}$ is not only very large near the crust-core interface but this property is, to a large extent, independent of an equation of state employed (derivatives of $n_a(r)$ grow in the vicinity of the crust for any equation of state), as well as on the configuration of the magnetic field (at least, for sufficiently large $\boldsymbol{B}$). Implication of these results is discussed in the next section.

4. Discussion and conclusions

The self-consistent method of calculation of $\partial_t\boldsymbol{B}$ for a given $\boldsymbol{B}$ in the quasistationarity approximation, was formulated in [5]. In this work it is further developed and applied to study

non-equilibrium processes induced in npe NS core by applied poloidal magnetic field. One of our main results is the analytic expression (6) for the meridional flow velocity $\boldsymbol{U}^{(p)}$. It is driven by frictional entrainment of neutrons by protons that interact with the magnetic field. The net flow of npe-fluid appears to be substantially larger than the diffusion flows of individual particle species. This result is of conceptual importance since it contradicts a standard point of view that the matter of neutron star cores, which is mainly composed of neutral particles, is (roughly) at rest in magnetized neutron stars (e.g., [4, 8]).

Comparing the terms $-c\,\mathrm{rot}\,\boldsymbol{E}_{\mathrm{com}}$ and $\mathrm{rot}\,[\boldsymbol{U}\times\boldsymbol{B}]$ in the Faraday equation (1d), and using the expression (5) for $\boldsymbol{E}_{\mathrm{com}}$, one can demonstrate that $c\,|\mathrm{rot}\,\boldsymbol{E}_{\mathrm{com}}| \ll |\mathrm{rot}\,[\boldsymbol{U}\times\boldsymbol{B}]|$ for $B \gtrsim 10^{13}$ G, provided that $w_a \ll U$. This means that a sufficiently strong magnetic field is frozen in the npe-fluid to a good approximation.

Let us consider several scaling relations for the quantities derived above. From equation (2) we obtain $\Delta\mu,\ \delta\mu_n \propto B^2$, where B is some typical value of the magnetic field in the core (e.g., $B_{\max}$). The n-p friction coefficient $J_{np} \propto \widetilde{T}^2$ and $\lambda \propto \widetilde{T}^6$ for modified Urca process (see [5], section VI). Then we have $U \propto B^2/\widetilde{T}^2$ in the low-temperature limit and $U \propto B^2\widetilde{T}^6$ in the high-temperature limit. Defining now the characteristic timescale of the field evolution as $\tau \sim B/\partial_t B \sim R/U$ and taking into account that the velocity U near the crust-core interface can be as large as $\sim 10^{-7}$ cm/s for $B \sim B_{\max} \approx 4.4\times10^{14}$ G and $\widetilde{T} \sim 2\times10^8$ K, we get the following estimate, valid in the low-temperature case

$$\tau \gtrsim (1-10)\,\mathrm{Myr}\left(\frac{\widetilde{T}_8}{B_{14}}\right)^2, \tag{11}$$

where $B_{14} = B/(10^{14}\,\mathrm{G})$ and $\widetilde{T}_8 = \widetilde{T}/(10^8\,\mathrm{K})$. Note that this is a timescale of nondissipative transformation of the magnetic field, in contrast to the timescale τ_{B}, defined in [5], which is purely dissipative. As one can see from this estimate, the typical evolution timescale for magnetars with the highest interior field $B \sim 10^{16}$ G [7] is of the order of $\sim 100-1000$ yr.

In the end let us mention that the approach to quasistationary evolution of the magnetic field developed here, can be extended in a number of ways. In particular, it can be generalized to include various additional particle species (e.g., muons and hyperons), baryon pairing, and non-axisymmetric magnetic field [5].

Acknowledgments

This work is supported by Russian Science Foundation (grant No. 14-12-00316). The authors are grateful to P S Shternin for criticism and to D G Yakovlev for encouragement.

References

[1] Viganò D, Rea N, Pons J A, Perna R, Aguilera D N and Miralles J A 2013 *MNRAS* **434** 123–141
[2] Bransgrove A, Levin Y and Beloborodov A 2018 *MNRAS* **473** 2771–2790
[3] Castillo F, Reisenegger A and Valdivia J A 2017 *MNRAS* **471** 507–522
[4] Passamonti A, Akgün T, Pons J A and Miralles J A 2017 *MNRAS* **465** 3416–3428
[5] Gusakov M E, Kantor E M and Ofengeim D D 2017 *Phys. Rev. D* **96**(10) 103012
[6] Braithwaite J and Spruit H C 2006 *A&A* **450** 1097–1106
[7] Beloborodov A M and Li X 2016 *ApJ* **833** 261
[8] Goldreich P and Reisenegger A 1992 *ApJ* **395** 250–258
[9] Yakovlev D G and Shalybkov D A 1990 *Soviet Astronomy Letters* **16** 86
[10] Reisenegger A 1995 *ApJ* **442** 749–757
[11] Yakovlev D G, Kaminker A D, Gnedin O Y and Haensel P 2001 *Phys. Rep.* **354** 1–155
[12] Heiselberg H and Hjorth-Jensen M 1999 *ApJL* **525** L45–L48
[13] Mereghetti S, Pons J A and Melatos A 2015 *Sp. Sci. Rev.* **191** 315–338
[14] Urpin V A and Ray A 1994 *MNRAS* **267** 1000